Published in final edited form as:
J Am Chem Soc. 2010 August 25; 132(33): 11443–11445. doi:10.1021/ja105108q.

Conserved binding mode of human β_2 adrenergic receptor inverse agonists and antagonist revealed by X-ray crystallography

Daniel Wacker[1,†], **Gustavo Fenalti**[1,†], **Monica A. Brown**[1,†], **Vsevolod Katritch**[2], **Ruben Abagyan**[2], **Vadim Cherezov**[1], and **Raymond C. Stevens**[1,*]

[1]Department of Molecular Biology, The Scripps Research Institute, La Jolla, CA 92037, USA

[2]University of California, San Diego, Skaggs School of Pharmacy and Pharmaceutical Sciences, La Jolla, CA 92093, USA

G protein-coupled receptors (GPCRs) are the largest protein family involved in signal transduction across membranes1. The β_2 adrenergic receptor (β_2AR) is one of the best characterized members of the GPCR family, for which pharmacologically distinct high-affinity ligands have been described as (i) agonists (compounds activating signaling), (ii) antagonists (blocking agonist signaling) or (iii) inverse agonists (blocking both agonist and basal signaling). The human β_2AR structure has previously been determined in complex with two partial inverse agonists, carazolol ($^{Car}\beta_2$AR-t4l)2 and timolol ($^{Tim}\beta_2$AR-t4l)3 and turkey β_1 adrenergic receptor has been determined in complex with the antagonist cyanopindolol4. A number of studies have used these structures for *in-silico* ligand docking and discovery of new scaffolds of β_2AR ligands5–8. Currently, a challenge for rational drug design and docking studies is to ascertain to what degree the conformation of the ligand binding site changes upon interaction with different compounds. To assess the extent of such ligand-induced conformational differences and reveal further details of ligand binding, we determined the X-ray crystal structure of β_2AR in complex with two of the most potent inverse agonists and the well known antagonist alprenolol.

Using a previously described engineered β_2AR construct3, the co-crystal structures of β_2AR-t4l in complex with **1** ($^{ICI}\beta_2$AR-t4l), **2** ($^{2}\beta_2$AR-t4l) and **3** ($^{Alp}\beta_2$AR-t4l) were determined at 2.8Å, 2.8Å and 3.1Å, respectively (Figure 1; see Supporting Information for experimental details). All three structures show the same overall fold observed for the previous $^{Car}\beta_2$AR-t4l and $^{Tim}\beta_2$AR-t4l structures with a rmsd of ~0.3Å (over β_2AR Cα atoms only) between all five reported β_2AR-t4l-ligand structures (Figure 2). Ligand mass spectrometry identification, receptor thermostability analysis, and the crystal structures reported here are consistent with the presence of compound **1**, **2** and **3** bound in each of the β_2AR-t4l complexes. The electron density shows the compounds bound to the same orthosteric binding site as carazolol and timolol, with minor differences in side chain orientations that reflect specific ligand-receptor interactions (Figure 2).

The binding pocket of β_2AR can be described as a narrow cleft surrounded by mostly hydrophobic residues, with few polar residues located at the `front' (Asp113$^{3.32}$, Tyr316$^{7.43}$ and Asn312$^{7.39}$) and `back' (Ser203$^{5.42}$, S207$^{5.46}$ and Asn293$^{6.55}$) of the binding site

* stevens@scripps.edu .
† These authors contributed equally to this work

Supporting Information Available: Supplementary experimental procedures, crystallographic data, structural figures and references (PDF). This material is available free of charge via the Internet at http://pubs.acs.org.

(Figures 1 and 2). Compounds **2**, **3**, carazolol and timolol contain an aliphatic oxypropanolamine moiety (compound **1** has a structurally similar oxybutanolamine), referred to as the ligand tail, and chemically and structurally diverse aromatic systems defined as the ligand head groups.

The amine and hydroxyl groups in the tails of **1**, **2** and **3** establish a conserved hydrogen bond network with the receptor polar triad Asp113$^{3.32}$, Tyr316$^{7.43}$ and Asn312$^{7.39}$ in the `front' of the pocket that closely resembles the ligand interactions observed in the $^{Tim}\beta_2$AR-t4l and $^{Car}\beta_2$AR-t4l structures (Figures 1 and 2). The aromatic head groups of the ligands, however, are mostly anchored between the side chains of Val114$^{3.33}$ and Phe290$^{6.52}$ in the `back' of the binding site, where each compound establishes distinct interactions with β_2AR (Figure 1).

Compared to carazolol, timolol and compound **2**, the dihydro-indene head group of the inverse agonist compound **1**9 is smaller and does not contain any polar groups that could accept or donate hydrogen bonds. The $^{ICI}\beta_2$AR-t4l structure shows the C4 carbon in the tail of compound **1** in the vicinity of Phe193$^{5.32}$, and the cyclopentene ring of the dihydro-indene in close proximity to the Phe289$^{6.51}$ and Phe193$^{5.32}$ sidechains in the `back' of the binding site (Figures 1 and 2). Furthermore, **1** has an additional methyl group on the aromatic system, and a comparison between all β_2AR-t4l-ligand structures shows that this compound requires some rearrangements in Ser203$^{5.42}$ (~1.2Å compared to other β_2AR-t4l structures) and a slight local shift ~0.4 Å in transmembrane helix 5 (TM V) (Figure 2).

The structure of $^{2}\beta_2$AR-t4l provides further structural insights into the binding mode of the strong inverse agonist compound **2**6. The geometry adopted by compound **2** in the active site of the $^{2}\beta_2$AR-t4l structure overlaps well with that of carazolol in the $^{Car}\beta_2$AR-t4l structure, and we also observe a hydrogen bond between the side chain of Ser203$^{5.42}$ (TM V) and the benzofuran oxygen O3 of compound **2** (Figures 1 and 2). In addition, the ethyl-carboxylate moiety extends towards Asn293$^{6.55}$ and allows for an additional hydrogen bond interaction between the oxygen O2 and the amine group of Asn293$^{6.55}$ side chain in TM VI (Figure 2). A comparison between the available crystal structures of β_2AR-ligand complexes reveals that compound **2** is the only ligand that connects TM V and VI through hydrogen bond networks. Other than a few minor differences, the compound 2 pose in the $^{2}\beta_2$AR-t4l structure is similar to that predicted by Kolb *et al.*6 with an rmsd of ~0.9Å.

Unlike compound **1**, **2**, timolol and carazolol, which contain at least one cyclic system other than the aromatic ring, the allylbenzene head group of the antagonist compound **3**10 is smaller and contains only a short prop-1-ene attached to the benzene group. Although the $^{Alp}\beta_2$AR-t4l structure has been determined at 3.1 Å resolution and therefore decreased confidence in the ligand placement (see Supplemental Material), there is sufficient electron density detail to orient the prop-1-ene chain of **3** in the same location as the cyclic system present on the other 4 compounds (Figure 2).

Although we observe a conserved binding mode for the β-hydroxy-amine motif on the ligand tails, a common feature among the `classical' scaffold of β_2AR ligands with inverse agonist, antagonist or full/partial agonist activities5, all β_2AR-t4l-ligand crystal structures show distinct interactions between the head groups of the ligands and the receptor (Figures 1 and 2). While the aromatic moieties of all compounds are anchored by strong hydrophobic interactions in the binding cleft, specific hydrogen bonds are also established by substituent moieties in compound **2,** timolol and carazolol.

Recently performed large scale docking and virtual screening studies6,11 suggest that the $^{Car}\beta_2$AR-t4l structure is highly efficient in screening for a wide range of antagonists and inverse agonists, though certain changes in the binding pocket may still be required for

optimal binding of high affinity agonists. Since almost identical conformations were found for the ligand binding site in all five β_2AR-t4l structures, we set out to investigate whether a single complex structure could be suitable for docking a range of antagonists and inverse agonists6,11. To test this hypothesis, we performed cross-docking experiments where each of the five ligands was docked into each β_2AR-t4l structure. The results (see Supporting Information) show excellent accuracy of docking pose predictions (rmsd<1Å) and high binding scores (ICM Score<−30 kJ/mol) for the docked compounds. The exception is compound **1**, which cross-docks poorly into all other crystal structures, mostly because of its exocyclic methyl group, which cannot be optimally accommodated within the slightly smaller pockets of the other structures. Overall, these results support the applicability of different β_2AR-ligand structures for docking and virtual screening of antagonists and inverse agonists. Substantially better binding scores for self-docking (except for compound **2**), however, suggest that additional ligand-receptor structures can further improve the performance of *in-silico* docking and can be particularly valuable for rational drug design at lead optimization stages.

Minimal structural differences between the three complexes reported here indicate that the ligands studied exert only minor local impact on the structure of the receptor. The most conserved region is the `front' part of the orthosteric binding pocket of the receptor, and therefore it is unlikely associated with distinct pharmacological properties of antagonists and inverse agonists. Instead, differences in specific interactions between the ligand and receptor TMs III, V and VI that take place through the aromatic ring system appear to define the pharmacologic effects. Note that agonists, characterized by a distinctly shorter “tail” and multiple polar substituents in the aromatic system are likely to introduce other changes in the β_2AR binding pocket associated with activation of the receptor, although the degree of these changes are yet to be structurally observed.

The result that β_2AR bound to pharmacologically distinct ligands (antagonists and inverse agonists) have virtually identical backbone conformations in the crystal structures suggests that the conformational changes capable of modifying signaling properties are very small, beyond the resolution of the obtained data. Alternatively, and more likely, the major effect of the antagonists/inverse agonists versus agonists in β_2AR is not on modifying a specific conformation but on changing the receptor dynamics. The answer to this intriguing problem should likely arrive from a combination of crystallography with techniques sensitive to dynamics, such as NMR12, EPR13, and HDX14.

Supplementary Material

Refer to Web version on PubMed Central for supplementary material.

Acknowledgments

The authors thank Kirk Allin, Ellen Chien and Tam Trinh for their valuable support with protein expression. We also thank Wei Liu for the help with LCP preparation, Michael McCormick for the support with data processing, Aaron Thompson and Mauro Mileni for helpful comments, Sunia Trauger at the Center for Mass Spectrometry at TSRI, Brian Shoichet and Peter Kolb at UCSF for coordinates of their compound 2 - receptor model, The Ohio State University, and Martin Caffrey, Trinity College (Dublin, Ireland), for the generous loan of the in meso robot (built with support from the National Institutes of Health [GM075915], the National Science Foundation [IIS0308078], and Science Foundation Ireland [02-IN1-B266]); and the staff at APS GM/CA for assistance with data collection. The GM/CA-CAT beamline (23-ID) is supported by the National Cancer Institute (Y1-CO-1020) and the National Institute of General Medical Sciences (Y1-GM-1104). This research was supported in part by the NIH Roadmap Initiative grant GM073197 for technology development and Protein Structure Initiative grant GM074961 for structure production. Coordinates and structure factors for the 3 complexes have been deposited in the RCSB Protein Data Bank with accession codes 3NY8, 3NY9, 3NYA.

REFERENCES

(1). Audet M, Bouvier M. Nat Chem Biol. 2008; 4:397. [PubMed: 18560432]

(2). Cherezov V, Rosenbaum DM, Hanson MA, Rasmussen SG, Thian FS, Kobilka TS, Choi HJ, Kuhn P, Weis WI, Kobilka BK, Stevens RC. Science. 2007; 318:1258. [PubMed: 17962520]

(3). Hanson MA, Cherezov V, Griffith MT, Roth CB, Jaakola VP, Chien EY, Velasquez J, Kuhn P, Stevens RC. Structure. 2008; 16:897. [PubMed: 18547522]

(4). Warne T, Serrano-Vega MJ, Baker JG, Moukhametzianov R, Edwards PC, Henderson R, Leslie AG, Tate CG, Schertler GF. Nature. 2008; 454:486. [PubMed: 18594507]

(5). Katritch V, Reynolds KA, Cherezov V, Hanson MA, Roth CB, Yeager M, Abagyan R. J Mol Recognit. 2009; 22:307. [PubMed: 19353579]

(6). Kolb P, Rosenbaum DM, Irwin JJ, Fung JJ, Kobilka BK, Shoichet BK. Proc Natl Acad Sci U S A. 2009; 106:6843. [PubMed: 19342484]

(7). Novoseletsky VN, Pyrkov TV, Efremov RG. SAR QSAR Environ Res. 2010; 21:37. [PubMed: 20373213]

(8). Vilar S, Karpiak J, Costanzi S. J Comput Chem. 2010; 31:707. [PubMed: 19569204]

(9). Devanathan S, Yao Z, Salamon Z, Kobilka B, Tollin G. Biochemistry. 2004; 43:3280. [PubMed: 15023079]

(10). Yao XJ, Velez Ruiz G, Whorton MR, Rasmussen SG, DeVree BT, Deupi X, Sunahara RK, Kobilka B. Proc Natl Acad Sci U S A. 2009; 106:9501. [PubMed: 19470481]

(11). Reynolds KA, Katritch V, Abagyan R. J Comput Aided Mol Des. 2009; 23:273. [PubMed: 19148767]

(12). Bokoch MP, et al. Nature. 2010; 463:108. [PubMed: 20054398]

(13). Altenbach C, Kusnetzow AK, Ernst OP, Hofmann KP, Hubbell WL. Proc Natl Acad Sci U S A. 2008; 105:7439. [PubMed: 18490656]

(14). Zhang X, Chien EY, Chalmers MJ, Pascal BD, Gatchalian J, Stevens RC, Griffin PR. Anal Chem. 2010; 82:1100. [PubMed: 20058880]

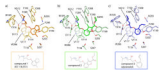

Figure 1.
Structural comparison of the ligand binding sites in the (a) $^{ICI}\beta_2$AR-t4l, (b) $^{2}\beta_2$AR-t4l and (c) $^{Alp}\beta_2$AR-t4l crystal structures. The ligands **1** (ICI 118,551), **2** and **3** (alprenolol) are colored in darker shades of orange, green and blue, respectively, while residues around the binding site are colored in lighter shades and labeled. Hydrogen bonds are depicted as black dotted lines. Chemical structures of compounds are shown in boxes.

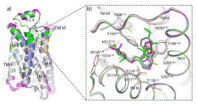

Figure 2.

Conserved overall fold of the $^{ICI}\beta_2$AR-t4l, $^{2}\beta_2$AR-t4l and $^{Alp}\beta_2$AR-t4l structures compared to $^{Tim}\beta_2$AR-t4l and $^{Car}\beta_2$AR-t4l. (a) Superimposition of all β_2AR-t4l crystal structures determined to date (t4l omitted); $^{ICI}\beta_2$AR-t4l (yellow), $^{2}\beta_2$AR-t4l (green), $^{Alp}\beta_2$AR-t4l (blue), $^{Tim}\beta_2$AR-t4l (magenta) and $^{Car}\beta_2$AR-t4l (grey) (b) Close view of the ligand binding site showing the conserved binding of the hydroxy-amine motif and the differences in the aromatic system moieties. Compounds are shown as sticks and surrounding residue side chains are shown as lines. Superscripts indicate the Ballesteros-Weinstein numbering convention.